

THE STATE SPACE MYSTERY WITH NEGATIVE LOAD IN MULTIPLE-VALUED LOGIC

Pavol GALAJDA¹⁾, Milan GUZAN²⁾, Viktor ŠPÁNY¹⁾

1) Department of Electronics and Multimedial Communications

2) Department of Theoretical Electrotechnics and Electrical Measurement
Technical University of Košice
Park Komenského 13, 041 20 Košice
Slovak Republic

Abstract

Switching sequential circuits are an indispensable part of many modern electronic devices, such as memory cells, flip-flop sensors, and many others. Since the invention of flip-flop switching circuits, the study of their dynamic behaviour has played an ever-increasing role. The dynamic properties of sequential circuits can be investigated by means of switching between the system's attractors. In this paper the boundary surfaces are discussed that play a crucial role in the process of switching.

Keywords

State space, boundary surface, control pulse, singularities, piecewise-linear approximation, eigenvalue

1. Introduction

The conference paper [4] about the multiple-valued memory using resonant tunneling diode (RTD) pair was the first work, which stimulated our research corresponding to circuits with negative load. The first information on their unique dynamic properties appeared as an internal announcement [1] and then as a paper in conference proceedings [3]. The exact dynamic properties of sequential circuits can be investigated by means of switching between the system's attractors. In this paper the morphology of boundary surfaces is discussed that play a crucial role in the process of switching. Multipeak resonant tunneling diode (RTD) properties caused our interest in these subjects. Resonant tunneling was found to be very promising in the design of new functional devices [7]. Practical circuits using a pair of multipeak RTD's yield the best result from the standpoint of size, power dissipation, and speed.

It is known that use of multivalued logic circuits can provide more information for each signal line, and reduce the number of interconnections within a chip or between chips [6]. For this system, it is desirable to have a high-density and high-speed multivalued static random-access memory (SRAM) to perform the function of storage. To increase the density of the memory, one way is to shrink the size of the memory cell itself, and the other approach is to implement a multistate memory cell. In this paper, a non-linear bias method is proposed to increase the number of states of multivalued memory cell.

The results in announcements [1], [2], and [3] were very interesting from mathematical point of view as well. Based upon these works we have derived new formulation of the conclusions, which were introduced in [9], [10], and [11]. They remain true only with respect to the positive load, so they are not general properties. The eigenvalues of the Jacobian matrix at the saddle equilibrium point have the property that exactly one of the mutually different eigenvalues of the Jacobian is real and positive. It is interesting to note that this eigenvalue property is shared by all sequential dynamic systems with linear load. Up to now, nobody tried to make the rigorous mathematical proof of this empirical postulate, although it should be of considerable interest in other fields also [18].

In the case when the device with negative resistance region is connected as a load for the active device, the eigenvalues at the saddle equilibrium point need not have the previously mentioned eigenvalue property. Consequently, it was not possible to find out the shape of the boundary surfaces, since their corresponding eigenspace, associated with the saddle equilibrium point, cannot be geometrically represented as it was first pointed out with respect to the positive load in [8]. The computer simulations, which detected the shape of the boundary surfaces, were first pointed out in conference paper [3]. Because in this case the boundary surface is like two-paraboloids in shape, the boundary surface element is the tangential plane in mutual point of these two paraboloids. That is the case to be outlined later.

While in the case of the positive load, the boundary surface element corresponds only to one real positive eigenvalue, in the case of the negative load, the boundary surface element corresponds to the dominant eigenvalue of the Jacobian matrix at the saddle equilibrium point [2].

Just as interesting are findings corresponding to the unstable limit cycle for negative load, which in this case is totally unstable. It means the unstable limit cycle is not an attractor for any initial conditions, so it is not saddle-type as in the case of positive load. The saddle-type unstable limit cycle in the case of positive load was

published for the first time in work [13] and later in paper [9].

The algorithm for calculation and delineation of boundary surfaces was published in [12], [13], [14], [15], and [16] in detail. The application of boundary surfaces for determination of the critical trigger pulse width were pointed out first in reference [15]. Papers [12], and [17] confirm the good agreement of experimental results with simulations on the computer of the response of the memory cell after introducing the trigger pulse.

2. Preliminary considerations

Let us consider an equivalent circuit of the memory cell, as shown in Fig. 1. We adopt the notation where the symbols for electrical quantities i_k , u_k correspond to a non-linear active element possessing a negative resistance region while i_l , u_l represent a non-linear and negative load. By the symbol ΔI in Fig. 1 and in system (1) is defined the ideal current source by means of which the triggering is controlled. The characteristics of the active and the load device are in Fig. 2 where $k=1$ and $k=2$ represent the load and active device, respectively.

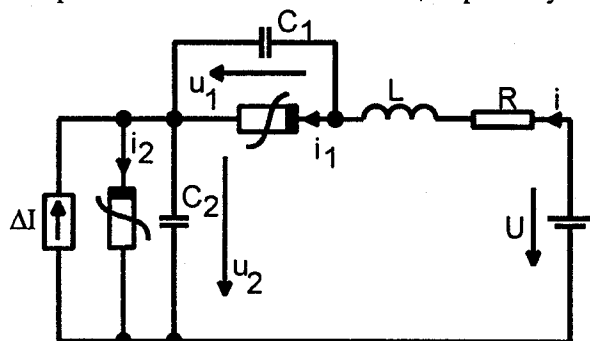


Fig. 1 Model of the memory cell

The state space model of the circuit in Fig. 1 is then given by the system

$$\begin{aligned} L \left(\frac{di}{dt} \right) &= U - Ri - (u_1 + u_2) \equiv Q_1 \\ C_1 \left(\frac{du_1}{dt} \right) &= i - f_1(u_1) \equiv Q_2 \\ C_2 \left(\frac{du_2}{dt} \right) &= i - f_2(u_2) + \Delta I \equiv Q_3 \end{aligned} \quad (1)$$

where the characteristic of the non-linear element $f_k(u_k)$ is defined [20] by the expression

$$\begin{aligned} f_k(u_k) = & \frac{1}{2} ({}^k g_0 + {}^k g_3) u_k + \frac{1}{2} [({}^k g_1 - {}^k g_0) u_k - {}^k U_1] + \\ & ({}^k g_2 - {}^k g_1) u_k - {}^k U_2 + ({}^k g_3 - {}^k g_2) u_k - {}^k U_3] - \\ & \frac{1}{2} [({}^k g_1 - {}^k g_0) {}^k U_1 + ({}^k g_2 - {}^k g_1) {}^k U_2 + ({}^k g_3 - {}^k g_2) {}^k U_3] \end{aligned} \quad (2)$$

while ${}^k g_i$ are the conductances and ${}^k U_i$ are the break points corresponding to segments of the characteristics as shown in Fig. 2. The I - V characteristic $f_k(u_k)$ for the active and load devices and for the case when $R=0$ (Fig. 1) are drawn in Fig. 6. The number of equilibria is defined by the right-hand sides of the Eq. (1) and the locations of the equilibria (co-ordinates, see Table 1) are given by the system of algebraic equations

$$Q_1 = 0, \quad Q_2 = 0, \quad Q_3 = 0, \quad (3)$$

The corresponding memory cell (Fig. 1) has five equilibria, three of which are sinks: $S1$, $S2$, $S3$. The remaining two equilibria $N1$ and $N2$ are saddle-type.

The control of the memory cell by means of the rectangular pulse with amplitude ΔI can be clarified as in references [9], [12] and [17].

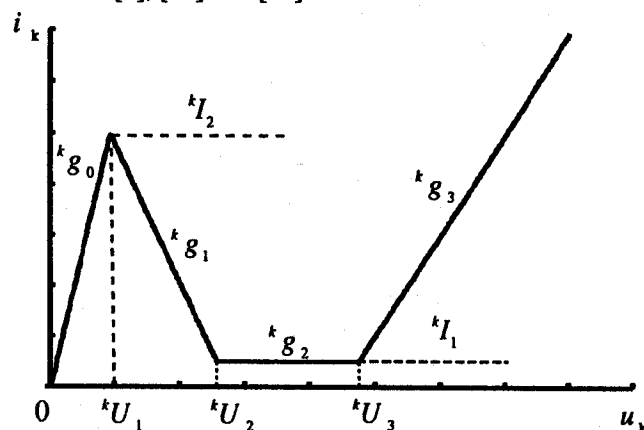


Fig. 2 Piecewise-linear approximation of the characteristics of the non-linear elements of the Fig. 1

In the sequential circuits investigated so far sequentiality was a sufficient condition for the existence of a boundary surface. Since in our case there exist attractors for sinks $S1$, $S2$, $S3$, and limit cycles $L1$, $L2$, $L3$ (Fig. 3 and Fig. 4), the existence of a boundary, corresponding to the saddle equilibrium points $N1$ and $N2$ is necessary if the existence and uniqueness of solutions of the system (1) are assumed. As the property of being sequential is shared by all memory cells, their dynamic properties can be investigated with the aid of boundary surface, regardless of whether they represent a binary or multi-valued logic. Of particular interest to us will be sets that separate attractors in the state space from each other.

On the basis of the introduced boundary surfaces it is possible to decide about the impulse magnitude and its duration so that the change of the information content in the elementary memory may occur.

The Jacobian matrix of the system (1) has the form

$$A = \begin{bmatrix} -\frac{R}{L} & -\frac{1}{L} & -\frac{1}{L} \\ \frac{1}{C_1} & -\left(\frac{{}^1 g_1}{C_1}\right) & 0 \\ \frac{1}{C_2} & 0 & -\left(\frac{{}^2 g_1}{C_2}\right) \end{bmatrix}. \quad (4)$$

The eigenvalues of the matrix A are defined by the determinant equation

$$\det |A - \lambda I| = 0 \quad (5)$$

where A is the matrix (4), λ is the eigenvalue of the matrix A and I is the unit matrix. The eigenvalues corresponding to equilibria defined by the system of algebraic equations (3) are listed in Table 1.

Linearizing (1) we get

$$\frac{d\bar{\Delta x}}{dt} = A\bar{\Delta x} \quad (6)$$

where $\bar{\Delta x} = (\Delta u_1, \Delta u_2, \Delta i)^T$ and $\bar{\Delta x} = \bar{x} - \bar{x}_s$,

while $\bar{x} = (u_1, u_2, i)^T$ and \bar{x}_s is the vector defining the coordinates of the equilibrium shown in Table 1.

Similarly the Jacobian matrix

$$A = \left. \frac{\partial \bar{Q}}{\partial \bar{x}} \right|_{\bar{x}=\bar{x}_s} \quad (7)$$

where $\bar{Q} = (Q_1, Q_2, Q_3)^T$.

After linear change of co-ordinates

$$\bar{y} = a\bar{\Delta x} \quad (8)$$

the system (6) becomes

$$\frac{d\bar{y}}{dt} = \Lambda \bar{y} \quad (9)$$

Here $\Lambda = \text{diag}(\lambda_1, \lambda_2, \lambda_3)$, so that particular solutions to (9) may be written in the form

$$\bar{y}(t) = \eta \bar{Y} \quad (10)$$

where $\bar{Y} = (Y_1, Y_2, Y_3)^T$ denotes the vector of initial conditions, and $\eta = \text{diag}(e^{\lambda_1 t}, e^{\lambda_2 t}, e^{\lambda_3 t})$.

From simulations it follows that the boundary surface element corresponds to the dominant eigenvalue [2] ($\text{Re}\{\lambda_i\} = \max(\{\text{Re}\{\lambda_i\}\}, i=1,2,3)$) of the Jacobian matrix at the saddle equilibrium point which, in view of (10), corresponds to the plane [8] and [12]

$$y_i = \alpha_{i1}\Delta u_1 + \alpha_{i2}\Delta u_2 + \alpha_{i3}\Delta i = 0 \quad (11)$$

(with the notation $\alpha = (\alpha_{ij})$).

Our change of co-ordinates (8) yields the matrix equation

$$aA - \Lambda a = 0 \quad (12)$$

the first row of which may be rewritten as

$$(A - \lambda_i I)^T \bar{a}_i = 0 \quad (13)$$

where $\bar{a}_i = (\alpha_{i1}, \alpha_{i2}, \alpha_{i3})^T$ is the eigenvector associated with the eigenvalue λ_i of A^T , and I is the unit matrix.

Since a matrix M and its transpose M^T have the same determinants, (13) has unique solution \bar{a}_i with $\alpha_{i3} = 1$.

The numerical values of the eigenvectors corresponding to the unstable equilibrium are shown in Table 1.

Table 1. The numerical values of the co-ordinates, eigenvalues and eigenvector for equilibria corresponding to memory cell in Fig.1. The bias voltage of the memory cell $U=440\text{mV}$; $L=1\text{e-}10\text{H}$; $C_1=C_2=5\text{e-}13\text{F}$; $R=0\Omega$. The parameter values corresponding to active and load device are as follows: $^1g_0=0,083$; $^1g_1=-0,057$; $^1g_2=0$; $^1g_3=0,028$; $^2g_0=0,1$; $^2g_1=0,05$; $^2g_2=0$; $^2g_3=0,03$ [S]; $^1U_1=60$; $^1U_2=130$; $^1U_3=280$; $^2U_1=50$; $^2U_2=140$; $^2U_3=260$ [mV].

Equilibrium	co-ordinates			eigenvector		
	u_1 [mV]	u_2 [mV]	i [mA]	α_{i1}	α_{i2}	α_{i3}
S1	385	54	4,5	*	*	*
N1	353	86	3,5	6,87221125	-0,787394	1
S2	275	164	1	*	*	*
N2	91	348	2,9	7,4171348	-0,9064227	1
S3	43	397	4,3	*	*	*
Equilibrium	eigenvalues					
	λ_{i1}			$\text{Re}\{\lambda_{i23}\}$	$\text{Im}\{\lambda_{i23}\}$	
S1	-123213594624			-53693206528	109004185600	
N1	31277887488			9461056512	195646275584	
S2	-32840130560			-15579936768	175476146176	
N2	25828651008			8985674752	198543147008	
S3	-145801281536			-55199363072	93755670528	

We apply the technique of graphical representation, via computer simulation, to explore the morphology of basins of attraction for the asymptotically stable states and the associated boundary surfaces. It is the latter that will concern us in this paper.

The basis for calculating and delineating boundary surface relative to non-linear load were papers [7], and [8].

3. Computer simulation results

The different techniques of computation and graphical representation of the boundary surfaces were outlined in papers [9], [10], [11] and [17]. Among the various numerical techniques of digital simulation we use the grid technique of basin delineation. This method does not require special knowledge but it demands the most of the computer time.

For example, we assume that the chosen grid is projected onto the (u_1, u_2) -plane (as shown in Fig. 3 and Fig. 4) for the cross section at level i , equal to the co-ordinate of the unstable equilibrium $N1$ and $N2$, respectively. To each sink corresponds a region, called the basin of attraction, of all points attracted toward the sink. The different colour areas represent the cross-section of these regions. The basin of attraction for sinks $S1$, $S2$, $S3$, and limit cycles $L1$, $L2$, $L3$ are delineated in Fig. 3 and Fig. 4 represented by the green, grey, red, yellow, pink and blue area respectively. For the given cross section (at $i=\text{constant}$ or $u=\text{constant}$ depending on the projection) these domains allow to decide what equilibrium state reaches the representative point of the trajectory after the pulse has been cancelled (Fig.5). Memory cell control is thoroughly described in Ref. [9], [11], [12], and [15] and here we shall only touch upon some aspects.

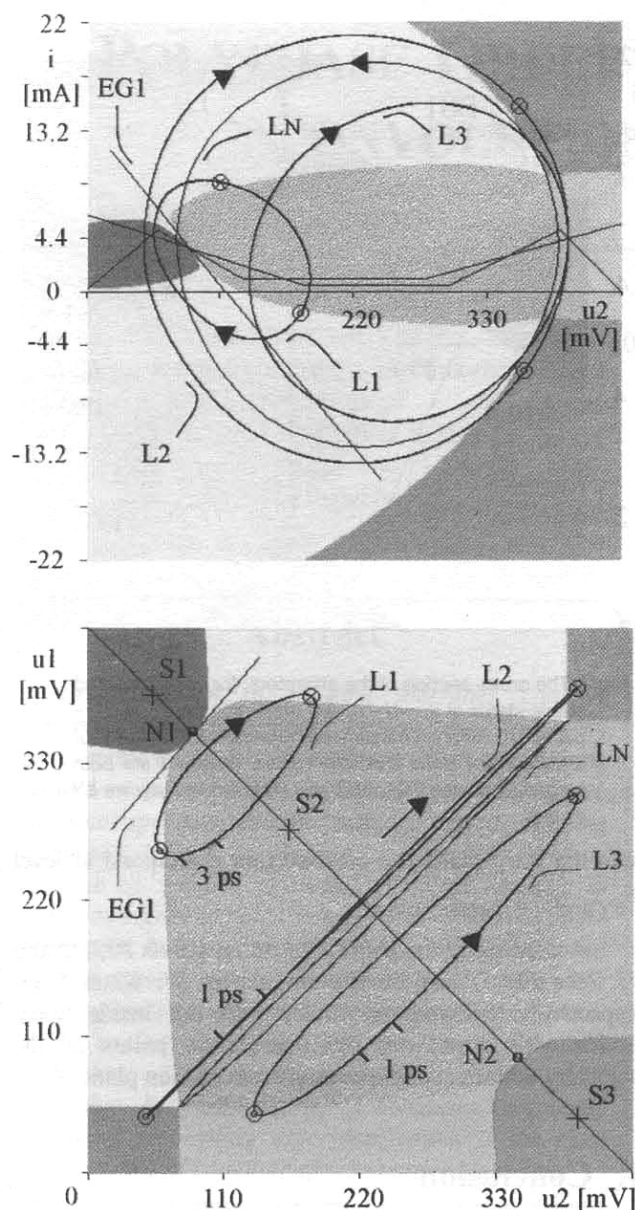


Fig. 3 Monge's projection of the cross-section (in singularity $N1$) of the boundary surfaces and stable limit cycles and unstable limit cycle.

Only the cases for the sequential circuits that have exactly one real positive eigenvalue of Jacobian A belonging to a saddle point have been published in papers [9], [10], [11], and [12]. This eigenvalue property is satisfied also for the four-dimensional state space published in [17]. Therefore the authors [17] suggested that this eigenvalue property for saddle points is shared by all sequential dynamical systems also in higher-dimensional state space. These conclusions were also based upon geometric delineation of boundary surfaces.

The case outlined here for geometric interpretation of the boundary surface is very interesting because saddle points $N1$ and $N2$ have all real positive eigenvalues. To this case corresponds also a very unusual shape of the boundary surfaces. This will be described for clarity only qualitatively and not exactly in Figures 3, 4, 5 and 6.

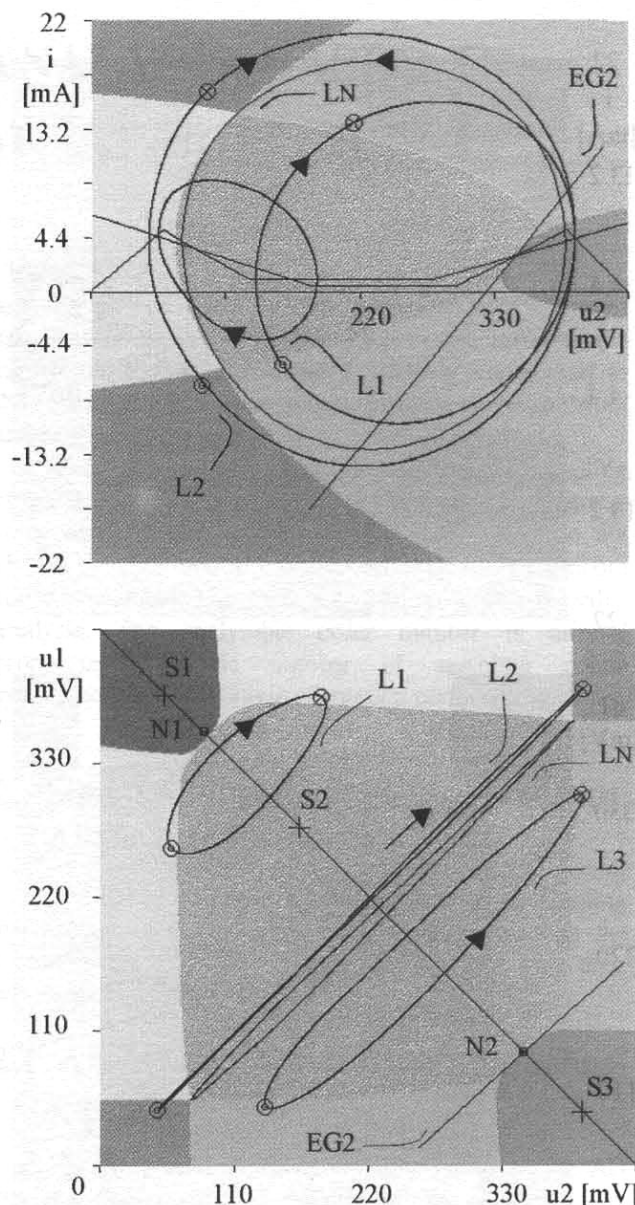


Fig. 4 Monge's projection of the cross-section (in singularity $N1$) of the boundary surfaces and stable limit cycles and unstable limit cycle.

The boundary surfaces corresponding to saddle point $N1$ and $N2$ are like two-paraboloids in shape. The cross-section for $N1$ and $N2$ is depicted as the border between the green \leftrightarrow yellow \leftrightarrow grey colour and between the grey \leftrightarrow blue \leftrightarrow red colour, respectively. Their common points are equilibria $N1$ and $N2$. The graphical representation of the cross-section of tangential planes $EG1$ and $EG2$ with the corresponding plane are shown in Fig.3 and Fig.4, respectively. In Fig.6 are depicted both tangential planes $EG1$ and $EG2$.

The singularity $S1$ is inside the green area, point $S2$ is inside the grey area and point $S3$ is inside the red area. In addition to the three above mentioned equilibrium states there are additional stable limit cycles $L1$, $L2$, $L3$ and one unstable limit cycles LN (see Fig.3 and Fig.4). It separates the state space (i, u_1, u_2) into six

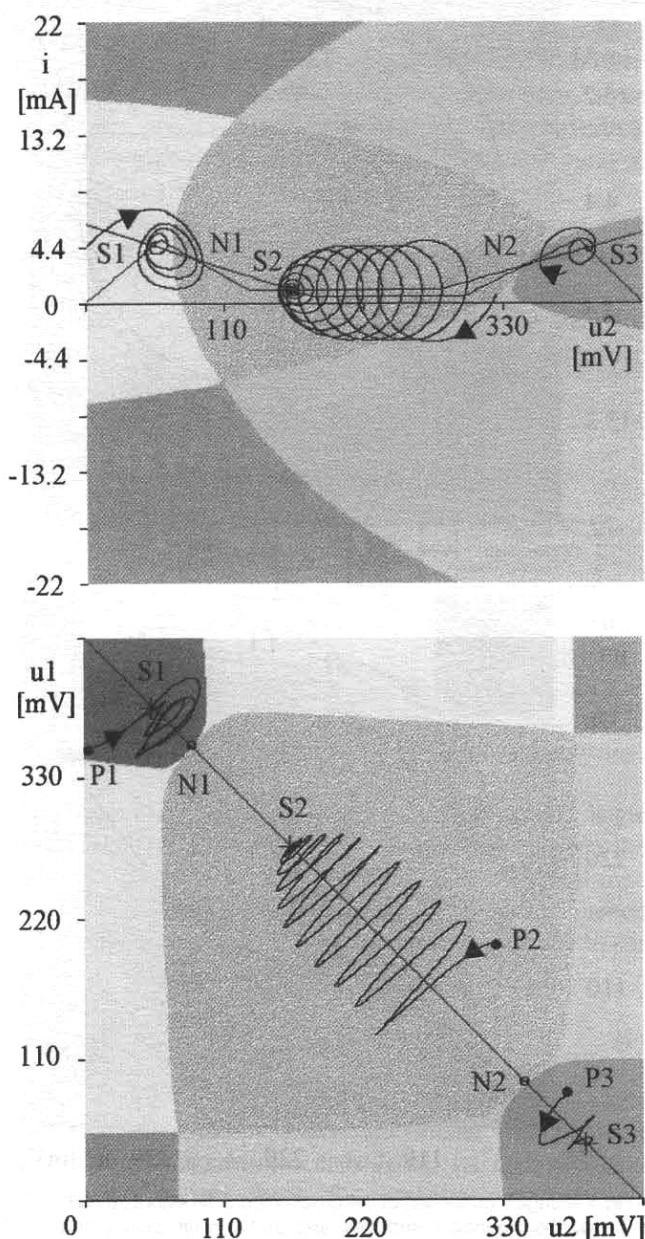


Fig. 5 Monge's projection of the cross-section of the boundary surfaces and the trajectories with initial conditions: $P1 (i = 4,4 \text{ mA}, u_1 = 352 \text{ mV}, u_2 = 1 \text{ mV})$, $P2 (i = 0,6 \text{ mA}, u_1 = 200 \text{ mV}, u_2 = 325 \text{ mV})$, $P3 (i = 0,24 \text{ mA}, u_1 = 80 \text{ mV}, u_2 = 380 \text{ mV})$.

domains of attraction. There is only one attractor (singularity $S1, S2, S3$ or limit cycles $L1, L2$ and $L3$) in each domain. Hence the initial conditions chosen in the particular domain lead to the corresponding attractor as shown in Fig. 5.

Monge's projection of the state space represents the exact solution of the system (1) with parameters, which are given in the text for Table 1. The cross-section corresponds to the singularities $N1$ and $N2$, i. e. in projection onto the (u_1, u_2) -plane the cross-section of the boundary surfaces are at level ^{N1}i and ^{N2}i , in the projection

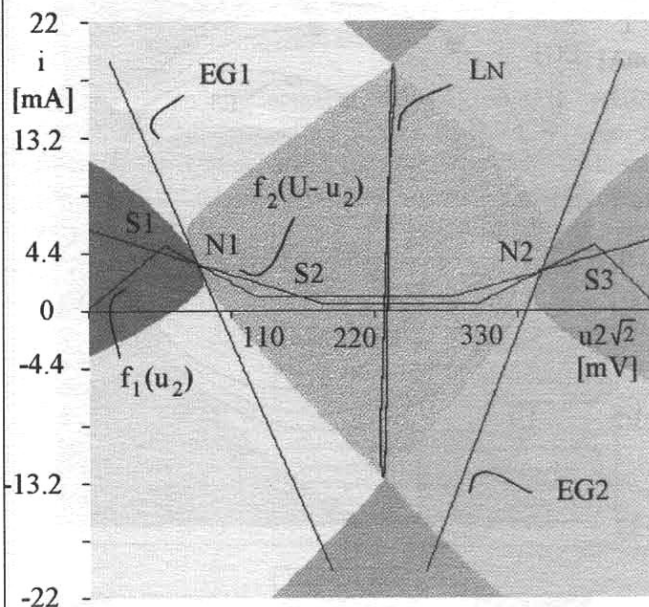


Fig. 6 The cross-section of the attractors, for corresponding stable states at $u_1 = U - u_2$ and projection onto $(i, u_2 \sqrt{2})$ -plane. The different colour areas represent the domains of attraction for sinks and limit cycles. Depicted are both tangential planes $EG1, EG2$ and unstable limit cycles LN as well.

onto the (i, u_2) -plane the cross-section correspond to level $^{N1}u_1$ and $^{N2}u_1$, respectively.

According to the above, the initial points $P1, P2$ and $P3$, (see Fig. 5) lead to the singularity $S1, S2$ and $S3$, respectively. Marked, as circles with dot inside (resp. circles with cross) are the intersection points of the trajectory with the corresponding cross-section plane.

4. Conclusion

The suggestion for this contribution was [4] and additional papers dealing with multiple valued logic, which relate to them. In the case when the device with negative resistance region is connected as a load for the active device, the eigenvalues of the Jacobian matrix A (4) at the saddle equilibrium point need not have exactly one real positive eigenvalue. The case outlined here is very interesting because saddle points have only real positive eigenvalues. The boundary surface exists while it has very strange shape from the geometrical viewpoint. It can be expected that the approach presented here will be applicable in multiple valued logic.

References

- [1] ŠPÁNY, V.: "Negative Load Resistance and the Basins of Attraction." Internal information in the Department of Radioelectronics, August 1994.

- [2] ŠPÁNY, V.: "The New Saddle Point and the Tangential Plane in this Singularity of the Boundary Surface." Internal information for Ph.D. students at the Department of Electronics and Multimedial Communications, November 1997.
- [3] ŠPÁNY, V.-GALAJDA, P.-GUZAN, M.: "Boundary Surfaces of One-port Memories." 5th International Conference Tesla Millennium, Beograd, October 15-18, 1996.
- [4] WEI, S. J.-LIN, H. CH.: "A Multi-State Memory Using Resonant Tunneling Diode Pair," 1991 IEEE International Symposium on Circuits and Systems, Singapore, June 1991, pp. 11-14.
- [5] LEON O. CHUA: "Chua's Circuit: A Paradigm for Chaos." World Scientific, 1997.
- [6] BUTLER, J., T.: "Multiple-valued logic. Potentials IEEE, April/May 1995, pp 11-14.
- [7] SEABAUGH, C., A.-KAO, Y., CH.-YUAN, H., T.: "Nine State Resonant Tunneling Diode Memory." IEEE Electron Device Letters, vol. 13, no. 9, September 1992, pp. 479-481.
- [8] ŠPÁNY, V.: "Graphical Solution of the Non-linear Circuit with the Help of the M-dimensional State Space." Elektrotechnický časopis, no. Č, vol. XX, pp. 233-248, in Slovak.
- [9] ŠPÁNY, V.-PIVKA, L.: "Boundary Surfaces in Sequential Circuits," International Journal of Circuit Theory and Applications, vol. 18, 1990, pp. 349-360.
- [10] ŠPÁNY, V.-PIVKA, L.: "Invariant Manifolds and Generation of Chaos," Elektrotechnický časopis, vol. 39, 1988, pp. 417-360.
- [11] ŠPÁNY, V.-PIVKA, L.: "2-Segment Bistability and Basin Structure in 3-Segment PWL Circuits," IEE Proceedings-G, Vol. 140, No. 1, Feb. 1993, pp. 61-67.
- [12] ŠPÁNY, V.-PIVKA, L.: "Boundary Surfaces and Basin Bifurcations in Chua's Circuit," Journal of Circuits, Systems and Computers, Vol. 3, No. 2, 1993, pp. 441-470.
- [13] ŠPÁNY, V.: "Special Surfaces and Trajectories of the Multidimensional State Space." Zborník VŠT v Košiciach 1, 1978, pp. 123-152, in Slovak.
- [14] ŠPÁNY, V.: "The Analysis of a One-tunnel Diode Binary." Proceeding IEEE 55, 1967, pp. 1089-1090.
- [15] ŠPÁNY, V.: "Trigger Pulse in a Circuit with Tunnel Diode." Slaboproudý obzor 26, 1965, pp. 246-247.
- [16] ŠPÁNY, V.: "The Simple VA Characteristic Approximation and the Complex Analysis of the Tunnel Diode Oscillator." Proceeding IEEE 55, 1967, pp. 1641-1643.
- [17] ŠPÁNY, V.-PIVKA, L.: "Boundary Surfaces in sequential circuits." Beitrage zur Theoretischeu Elektrotechnik, Das Internationale Symposium in Ilmenau, 1988, pp. 90-99.
- [18] GALAJDA, P. - ŠPÁNY, V.: "The Second Order Non-linear System, Applied in the Circuit Theory." Proceedings of the

scientific conference with international participation. Informatics and mathematics. September 4-5, 1997, Slovakia

- [19] Galajda, P.: "The Analysis of the Multiple-Valued Memory Cell," PhD. thesis, 1995, in Slovak.
- [20] ŠPÁNY, V.: "The Expression of the Non-Linear Characteristics by Means of Absolute Values," Slaboproudý obzor, Vol. 40, No. 7, 1988, pp. 354-356, in Slovak.

About authors...

Pavol GALAJDA was born in 1963 in Košice, Slovak Republic. He received the Ing. (M.Sc.) degree in electrical engineering from the FE TU in Košice and CSc. (Ph.D.) degree in radioelectronics from FEI TU in Košice, in 1986 and 1995, respectively. At present he is an assistant professor at the Department of Electronics and Multimedial Communications, FEI TU in Košice. His research interest is in nonlinear circuits theory and multiple-valued logic.

Milan GUZAN was born in 1969 in Snina, Slovak Republic. He received the Ing. (M.Sc.) degree in electrical engineering from the FE TU in Košice, in 1992. At present he is an assistant professor at the Department of Theoretical Electrotechnics and Electrical Measurement. His research interest is in multiple-valued logic and sensors based on multiple-valued memories.

Viktor ŠPÁNY (Prof., Ing., DrSc.), received his DrSc (PhD) degree from the Slovak University of Technology in Bratislava, Czechoslovakia. After joining the University of Technology in Košice in 1952 his research was devoted to pulse circuits and digital electronics. The result of these activities, published in local and international journals, have been summarized in the book Bipolar Transistor in Pulse Circuits. He directed his further activities toward numerical and graphical solutions of non-linear dynamical systems. Among the most important results were the algorithms for construction and utilization of boundary surfaces in flip-flop circuits and oscillatory systems. Currently he is Professor Emeritus of electrical engineering at the Department of Electronics and Multimedial Communications, Technical University in Košice, Slovakia.